

**Figure 4.** Western blot analysis of brush border membranes and SLPs isolated from the intestine of rat fed with corn oil using SLP antibodies. STOM, Stomach; COL, Colon; KID, Kidney.

A.M. a few microlitres of rat albumin antibodies, which were utilized for Western blot analysis using SLP proteins along with the standard rat albumin. To our surprise, all 4–6 SLP protein bands were strongly identified by rat albumin antibodies. A reverse experiment was also carried out, where using SLP antibodies, rat albumin was identified by Western blot analysis. Experiments were repeated using human albumin antibodies against human albumin and SLPs isolated from the human intestine. Essentially, similar results were obtained.

Amino acid analysis of the protein samples also showed that ten N-terminal amino acids (Asp–Ala–His–Lys–Glu–Val–Ala–His–Arg–Phe) were of albumin. This was further confirmed by a review of literature<sup>8,9</sup>. The amino acid sequence of the proteins

matched exactly with those reported in the literature<sup>8,9</sup>. Thus the nature of these novel proteins was solved after nearly 10 years of discovery of SLPs.

With the knowledge that albumin is a part of SLPs in association with AP (they have similar molecular mass; 64–65 kDa), some new questions arise. For example, what are the functions of albumin in SLPs? It is well known that albumin can bind to many ligands, including a variety of lipids, bile salts/pigments, toxins and metal ions. Thus a new chapter has begun to define the role of albumin in the intestine. The role of serum albumin in intestine can be further explore the significance of SLPs upon fat-feeding.

- Is there a separate lipid absorption pathway involving albumin in the intestine?
- Is it involved in the absorption of other ligands which bind to albumin in the intestine?
- What is its association with AP in the intestinal absorption of fats?
- What is its significance in adherence to other basolateral proteins?

These and many more questions will need answers in the future.

1. Eliakim, R., Deshryver-Keesckemetic, K., Nagee, L., Stenson, W. F. and Alpers, D. H., *J. Biol. Chem.*, 1989, **264**, 20614–20619.
2. Deshryver-Keesckemetic, K., Elaikim, R., Carrol, S., Stenson, W. F., Moxley, M. A. and

Alpers, D. H., *J. Clin. Invest.*, 1989, **84**, 1355–1361.

3. Mahmood, A., Yamagishi, F., Elaikim, R., Deschryver-Keesckemetic, K., Gramlich, T. L. and Alpers, D. H., *J. Clin. Invest.*, 1994, **93**, 70–80.
4. Mahmood, A., Mahmood, S., DeSchryver-Keesckemetic, K. and Alpers, D. H., *Arch. Biochem. Biophys.*, 1993, **300**, 280–286.
5. Engle, M. J., Mahmood, A. and Alpers, D. H., *Biochim. Biophys. Acta*, 2001, **1511**, 369–380.
6. Goetz, G. S., Mahmood, A., Hultgren, S. J., Engle, M. J., Dodson, K. and Alpers, D. H., *Infect. Immun.*, 1999, **67**, 6161–6163.
7. Mahmood, A., Engle, M. J., Hultgren, S. J., Goetz, G. S., Dodson, K. and Alpers, D. H., *Biochim. Biophys. Acta*, 2000, **1523**, 49–55.
8. Meloun, B., Moravek, L. and Kostka, V., *FEBS Lett.*, 1975, **58**, 134–137.
9. Isemiva, S. and Ikenaka, T., *J. Biochem.*, 1978, **83**, 35–48.

**ACKNOWLEDGEMENT.** We thank Professor D. H. Alpers, Washington University Medical School, St Louis, MO, USA for useful suggestions.

Received 1 June 2022; revised accepted 15 August 2022

AKHTAR MAHMOOD\*  
SHABEER AHMAD RATHER

*Department of Biochemistry,  
Panjab University,  
Chandigarh 160 014, India*

*\*For correspondence.  
e-mail: akhtarmah@yahoo.com*

## Modelling electric permittivity of ice–rock mixtures and implications regarding permittivity-based ice detection techniques in the 1–1000 Hz range

Potential resources for future lunar exploration can be identified and further quantified by studying the near-surface structure of the Moon, up to depths of hundreds of metres. The thermal and geological history of the Moon can also be deciphered from such studies. The lunar volatiles are expected to be preserved in cold traps or buried beneath the surface layer near the poles<sup>1</sup>. The Moon was considered to be entirely dry after the lunar sample return missions

(Apollo, Luna) in the 1960s and early 1970s. Infrared mapping by the Moon Mineralogy Mapper (M<sup>3</sup>) on Chandrayaan-1 resulted in the detection of hydroxyl molecule (OH) and water on the uppermost few millimetres of the lunar surface<sup>2</sup>. Recent efforts to study the lunar subsurface include various instruments such as the Kaguya lunar radar sounder<sup>3</sup> (LRS), the Chang-E1 microwave radiometer<sup>4</sup>, Mini-SAR<sup>5</sup> on-board Chandrayaan-1, Lunar Reconnaissance

Orbiter<sup>6</sup> (LRO) and DFSAR<sup>7</sup> on-board Chandrayaan-2 orbiter. This study presents the characterization of ice embedded in regolith materials and discusses a model for evaluating the real component of electric permittivity for the lunar subsurface. The frequency dependence of the real component of the electric permittivity is determined at temperatures 190 and 220 K, over a frequency range 1 Hz to 1 kHz for pure ice. The electric permittivity of two-component

ice–rock mixtures is calculated for various ice concentrations. The implications for the detection of lunar ice on the basis of permittivity-based probes are presented below.

The dielectric constant of dry materials is typically between 1 and 5. However, the permittivity of water is a function of frequency and temperature<sup>8</sup>. Both mutual impedance probe and ground-penetrating radar measurements can thus differentiate the electric permittivity of water from other materials since for static fields, the permittivity value is almost two orders of magnitude compared to that value for extremely high frequencies, and because permittivity varies with frequency and temperature. At very high frequencies, the molecules have no time to change their orientation in response to the applied electric field resulting in low dipolar polarizability (and dielectric constant)<sup>9</sup>, whereas in a static field, the polar molecules will prefer a slight orientation parallel to the applied field.

It is customary to characterize a dielectric using a complex dielectric constant (or permittivity)  $\epsilon$  in the following manner

$$\epsilon^*(f) = \epsilon'(f) - j\epsilon''(f), \quad (1)$$

where  $f$  is the frequency and  $j = \sqrt{-1}$ .  $\epsilon'$  is the real permittivity (or dielectric constant) and is one of the parameters used for characterizing electrical properties of materials. The general expression for complex permittivity (dielectric constant) is given by the Debye equation

$$\epsilon^* = \epsilon'_\infty + (\epsilon'_s - \epsilon'_\infty)/(1 + j\omega\tau), \quad (2)$$

where  $\epsilon'_s$  and  $\epsilon'_\infty$  are the static and high frequency limits of  $\epsilon$ .  $\omega$  and  $\tau$  are the angular frequency ( $2\pi f$ ) and Debye relaxation time constant respectively. If eq. (2) is separated into real and imaginary parts, the real part of the dielectric constant is obtained as

$$\epsilon' = \epsilon'_\infty + (\epsilon'_s - \epsilon'_\infty)/(1 + \omega^2\tau^2). \quad (3)$$

Petrenko and Whitworth<sup>10</sup> suggest that for pure ice, the high frequency limit ( $\epsilon'_\infty$ ) of the dielectric constant is  $\sim 3.15$  over a temperature range 200–260 K. Using the experimental data for permittivity for pure ice<sup>11</sup>, the following expression can be used for estimating the low frequency limit of permittivity

$$\epsilon'_s = 431 - 2.325T + 0.0041T^2, \quad (4)$$

where  $T$  is the temperature (K). The relaxation time constant  $\tau$  can be determined

using the expression derived from an earlier study by Kawada<sup>12</sup>.

$$\log(\tau) = -8.344 + 1.333(1000/T). \quad (5)$$

The real component of the electric permittivity for pure (100%) ice can be determined by estimating  $\tau$  and  $\epsilon'_s$  from the above equations and then applying eq. (3), while assuming  $\epsilon'_\infty = 3.15$ . Figure 1 shows a plot of the electric permittivity for pure ice as a function of frequency for two temperatures, i.e. 190 and 220 K. At 190 K the permittivity values for pure ice decrease from  $>100$  to around 3 between the frequency range 2 and 100 Hz, whereas for a temperature of 220 K, the electric permittivity is  $>100$  until  $\sim 10$  Hz and then exhibits a continuous decrease with frequency between 10 and 1000 Hz. Thus, we infer that the frequency dependence of the real component of electric permittivity permits detection of pure ice by measuring electric permittivity between 1 Hz and a few hundred Hertz.

The earlier discussion relates to determination of the permittivity for pure ice. However, if one considers the lunar surface, ice is likely to be mixed with regolith (primarily basaltic or anorthositic rocks). In this situation, the electric permittivity of a mixture is a nonlinear combination of relative fractions of various individual components. Landau and Lifshitz<sup>13</sup> have proposed that the permittivity of a mixture can be expressed as follows

$$3\sqrt{\epsilon} = \sum_i w_i \times \sqrt[3]{\epsilon_i}, \quad (6)$$

where  $w_i$  and  $\epsilon_i$  are the relative concentration and electric permittivity respectively, of different components in the mixture. We now consider a mixture of ice and lunar

regolith, and determine the electric permittivity for the two-component mixture at a temperature of 220 K. Fa and Wieczorek<sup>14</sup> have estimated the real part of the electric permittivity to vary from 2.5 to 3.4 over the entire lunar surface. We assume the real component of permittivity for the lunar regolith to be  $\sim 2.9$ , whereas the permittivity values for pure ice are estimated using eq. (3) for various concentrations, while assuming a temperature of 220 K. The ice concentration in the two-component mixture is then varied from 0.5% to 20% of the volume.

Figure 2 shows the (real) permittivity values for various ice–rock concentrations over a frequency range 1–1000 Hz. For 20%, 10% and 5% (water) ice content, the permittivity values change by  $\sim 220\%$ ,  $\sim 90\%$  and  $\sim 40\%$  respectively between 1 and 1000 Hz. For 2% ice content, the value of permittivity estimated for the ice–rock mixture is 3.34 at 1 Hz and 2.90 at 1000 Hz. Thus, the total change in permittivity is only 15% over a frequency range 1–1000 Hz for 2% ice concentration. The difference in permittivity between 1 and 1000 Hz reduces further for 1% and 0.5% ice concentrations, and is estimated to be around  $\sim 7\%$  and  $\sim 3.5\%$  respectively. The popular Maxwell Garnet<sup>15</sup> and Lichtenecker<sup>16</sup> models are used here to compare the above results for 5% ice concentration. As shown in Figure 3, the Landau–Lifshitz approximation provides an effective permittivity about  $\sim 20\%$  higher in comparison to the Maxwell Garnet model between 1 and 10 Hz, whereas at higher frequencies beyond  $\sim 150$  Hz, all three formalisms provide similar values of effective permittivity. It may be noted here that the Lichtenecker and Maxwell Garnet-based values of effective permittivity are similar

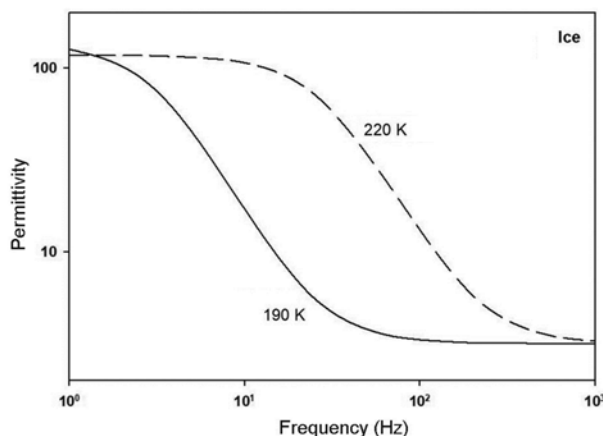
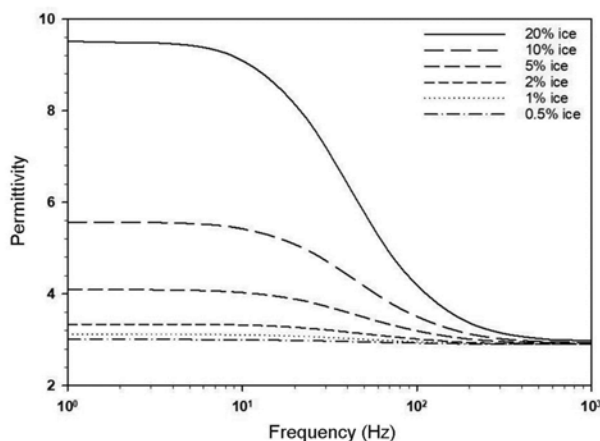
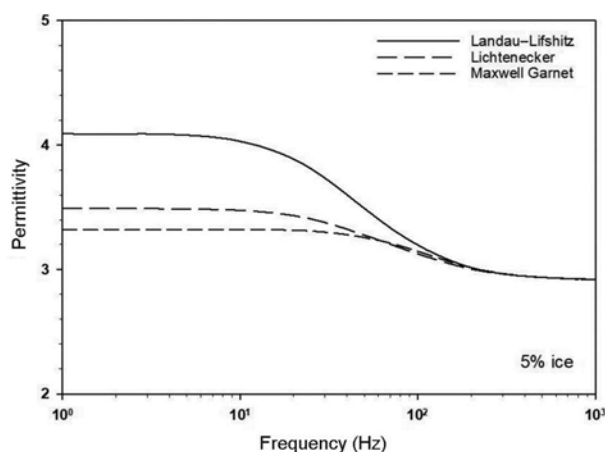


Figure 1. Variation of real part of electric permittivity for pure ice as a function of frequency for two temperatures (190 and 220 K).



**Figure 2.** Permittivity (real part) model for various mixtures of rock–ice concentrations in the frequency range 1–1000 Hz, determined using the Landau–Lifshitz mixing model. The temperature is assumed to be 220 K.



**Figure 3.** Comparison of effective permittivity values at 220 K for a 5% ice concentration, estimated using various mixing models (Landau–Lifshitz, Lichtenecker and Maxwell Garnett).

within the entire range of 1–1000 Hz, and are observed to be within ~5% of each other (Figure 3). Mutual impedance probes<sup>17</sup> measuring permittivity have been flown previously on the Huygens Probe which landed on Titan in 2005 (ref. 18). They usually comprise two transmitting electrodes and two receiving electrodes, and while a known current from the transmitting electrodes passes through the medium, the potential difference (voltage) between the two receiving electrodes is measured. The permittivity of the unknown medium is esti-

mated by measuring the amplitude and phase of the induced voltage in vacuum and in the unknown medium<sup>17</sup>. In light of the above calculations for permittivity of ice–rock mixtures, any mutual impedance probe proposed for a lunar lander (or rover) with an objective of ice detection requires to demonstrate a sensitivity for detecting permittivity variations of around a few per cent over the frequency range 1–1000 Hz, if ice concentration in the landing site is observed to be  $\leq 1\%$ . For higher concentrations of water ice, our modelling calculations show

that the presence of ice can be revealed clearly from the frequency dependence of the real component of electric permittivity.

1. Watson, K., Murray, B. C. and Brown, H., *J. Geophys. Res.*, 1961, **66**, 3033–3045.
2. Pieters, C. *et al.*, *Science*, 2009, **326**, 568–572.
3. Ono, T. *et al.*, *Science*, 2009, **323**, 909–912.
4. Fa, W. and Jin, Y. Q., *J. Geophys. Res.*, 2007, **E05003**, 112.
5. Spudis, P. D. *et al.*, *Geophys. Res. Lett.*, 2010, **37**, L06204.
6. Nozette, S. *et al.*, *Space Sci. Rev.*, 2010, **150**, 285–302.
7. Bhiravarasu, S. S. *et al.*, *Planet. Sci. J.*, 2021, **2**, 134.
8. Carmichael, R. S., *Practical Handbook of Properties of Rocks and Minerals*, CRC Press, Boca Raton, Florida, 1989, 1st edn, p. 756.
9. Kittel, C., *Introduction to Solid State Physics*, John Wiley, USA, New York, 1976, 5th edn, p. 599.
10. Petrenko, V. F. and Whitworth, R. W., *Physics of Ice*, Oxford University Press, Oxford, 1999, p. 390.
11. Johari, G. P. and Whalley, E., *J. Chem. Phys.*, 1981, **75**, 1333–1340.
12. Kawada, S., *J. Phys. Soc. Jpn.*, 1986, **44**, 1881–1886.
13. Landau, E. D. and Lifshitz, E. M., *Electrodynamics of Continuous Media*, Pergamon, New York, USA, 1960, 1st edn, p. 475.
14. Fa, W. and Wiczorek, M. A., *Icarus*, 2012, **218**, 771–787.
15. Maxwell Garnett, J., *Trans. R. Soc. London*, 1904, **203**, 385–420.
16. Lichtenecker, K., *Phys. Z.*, 1926, **27**, 115–158.
17. Trautner, R., Grard, R. and Hamelin, M., *J. Geophys. Res.*, 2003, **108**(E10), 8047.
18. Hamelin, M. *et al.*, *Adv. Space Res.*, 2000, **26**, 1697–1704.

Received 20 June 2022; revised accepted 22 August 2022

DEBABRATA BANERJEE

*Planetary Sciences Division,  
Physical Research Laboratory,  
Ahmedabad 380 009, India  
e-mail: deba@prl.res.in*